# Phytochemical characterization and anti-arthritic potential of *Croton bonplandianus* leaves extract: In-vivo and in-silico approach

Erum Javed [a], Humaira Majeed Khan [a,*], Qumar Shahzad [a], Yasser Shahzad [b,c,i,*], Hina Yasin [d], Zaheer Ul-Haq [e], Mobina Manzoor [f], Muhammad Usman Ghori [g], Amer M. Alanazi [h], Azmat Ali Khan [h]

[a] *Institute of Pharmacy, Faculty of Pharmaceuticals & Allied Health Sciences, Lahore College for Women University, Lahore 54000, Pakistan*
[b] *Department of Pharmacy, COMSATS University Islamabad, Lahore Campus, Lahore 54000, Pakistan*
[c] *Center of Excellence for Pharmaceutical Sciences, Faculty of Health Sciences, Private Bag X6001, Potchefstroom 2520, South Africa*
[d] *Department of pharmacognosy, Dow college of Pharmacy, Dow University of Health Sciences, Ojha campus, Karachi, Pakistan*
[e] *Dr. Panjwani Center for Molecular Medicine and Drug Research, International Center for Chemical and Biological Sciences, University of Karachi, Karachi 75270, Pakistan*
[f] *Punjab University College of Pharmacy, University of the Punjab, Lahore, 54000, Pakistan*
[g] *Department of Pharmacy, University of Huddersfield, Huddersfield HD1 3DH, UK*
[h] *Pharmaceutical Biotechnology Laboratory, Department of Pharmaceutical Chemistry, College of Pharmacy, King Saud University, Riyadh 11451, Saudi Arabia*
[i] *Faculty of Pharmacy, Universiti Sultan Zainal Abidin, Besut Campus, Besut 22200, Terengganu, Malaysia*

A R T I C L E   I N F O

A B S T R A C T

*Croton bonplandianus*, a natural source traditionally used for treating various illnesses, including rheumatoid arthritis, was evaluated in this study. The effects of ethanolic extracts (CBEE) and aqueous fractions (CBAF) of *C. bonplandianus* leaves on arthritis-induced inflammation were studied using an albino rat model of inflammation induced by Freund's complete adjuvant. Eight test groups (n = 5 per group) and one vehicle control were used to evaluate the antiarthritic effects of different doses of CBEE and CBAF (125 mg.kg$^{-1}$, 250 mg.kg$^{-1}$, and 500 mg.kg$^{-1}$) on days 5, 10, 15, and 20 compared to arthritic and vehicle controls. Arthritis severity was assessed using macroscopic arthritis grading, histological analysis, body weights, and paw thickness. CBEE and CBAF were found to reduce the prevalence of arthritis, increase body weight, and decrease paw inflammation compared to the vehicle control group by the 23rd day. In addition, they showed no effect on biochemical parameters, but a significant difference (p < 0.05) in hematological parameters compared to the arthritic control group. The study identified Hentriacontane compound as a potential contributor to the anti-inflammatory effect of *C. bonplandianus*, as it showed the lowest dock score for IL-1β and IL-6. Palmitoylethanol amide was identified as a potential contributor to the anti-inflammatory effect of TNF-α. Gene expression of IL-6, IL-1β, and TNF-α was down-regulated significantly (p < 0.05) in a dose-dependent manner in all treatment groups compared to the arthritic control group. In conclusion, this study validated the anti-arthritic and anti-inflammatory properties of CBEE and CBAF in a time and dose-dependent manner.

## 1. Introduction

Inflammation is associated with the occurrence of several chronic diseases, including atherosclerosis, rheumatoid arthritis, asthma, edema, gastric intolerance, tuberculosis, and bone marrow depression (Weber et al., 2023; Yasin et al., 2021). Several anti-inflammatory treatments, such as aspirin, indomethacin, phenylbutazone (Rainsford, 2007), as well as commonly used nonsteroidal anti-inflammatory drugs (NSAIDs) (Yasin et al., 2019), are used. However, despite their extensive use for symptomatic relief, NSAIDs have also been associated with several side effects (Simon, 2013), including gastrointestinal distress, colitis, acute renal failure, gastric or duodenal ulcer, small bowel erosion, hypertension, chronic kidney disease, heart failure, myocardial infarction, seizures, stroke, and delayed wound healing (Wongrakpanich

et al., 2018).

Rheumatoid arthritis (RA), characterized by chronic inflammation, is a multifactorial autoimmune disease that affects multiple joints over time (Lin et al., 2020). Its global prevalence is 1 % of the population. RA affects females two to three times more often than males of any age; however, it is most prevalent in people over 50 (Mateen et al., 2016; Woude et al., 2018). The factors used to characterize RA include rheumatoid factor and anti-citrullinated peptide antibodies, as well as initial stage activation of both B and T cells (Mateen et al., 2016). RA could be caused due to a combination of genetic, epigenetic, ecological influences such as dust, cigarette smoke, and the internal environment, which is the gut microbiome (Scherer et al., 2020).

The phytotherapy has been used for treating the inflammation since ancient times. Plant extracts and their agents are considered safer with limited side effects compared to drug molecules (Yasin et al., 2021). The Euphorbiaceae plant family is extensively used for cancer, diabetes, arthritis, liver, heart, and chest diseases, as well as infections (Sangha & Gayatri, 2014). The plant *Croton bonplandianus* (*C. bonplandianus*), a member of the Euphorbiaceae family, is an exotic weed also known as the three-leaved caper (Bar & Bar, 2020). *C. bonplandianus* is native to southern Bolivia, Paraguay, southern Brazil, northern Argentina, Bangladesh, South America, India, and Pakistan. (Ghosh, Kumar Biswas, et al., 2018). Several studies have been conducted to evaluate the therapeutic potential of *C. bonplandianus*'s leaves, fruits, latex, seeds, and baill. These studies evaluated the therapeutic potential of ethanolic, methanolic and dichloromethane extracts of *C. bonplandianus* for α-glucosidase inhibition (Qaisar et al., 2014), anti-cancer activity (Ajoy & Padma, 2013), genotoxic and antibacterial activity (Bar & Bar, 2020; Saggoo et al., 2010), hemolytic activity (Ghosh, Biswas, et al., 2018), anthelmintic activity (Singha et al., 2022) and anti-inflammatory activity (Sudha, 2021). However, very limited studies of ethanolic extract and aqueous fraction of leaves of *C. bonplandianus* against arthritis were reported. This study aims to evaluate the therapeutic potential of the ethanolic extract and aqueous fraction of *C. bonplandianus* leaves against rheumatoid arthritis (RA) in animal models. Additionally, mass-spectrometric analysis and molecular modeling of identified compounds were performed to identify potential binding target sites.

## 2. Materials and methods

### 2.1. Collection of the plant and extracts preparation

The *Croton bonplandianus* plant, a member of Euphorbiaceae family, was collected from the botanic garden of the University of Karachi. After adequate cleaning, 1000 g of collected leaves of *C. bonplandianus* were weighed. The leaves were percolated in 3.6 L of ethanol for 15 days at room temperature with intermittent shaking and filtered with Whatman filter paper. The excess solvent (ethanol) was then extracted under low pressure (at 40 °C temperature) in a rotary evaporator. This procedure yielded 656 g of ethanolic extract, and 500 g of the ethanolic extract was subjected to fractionation, while the remaining 156 g was lyophilized and used for phytochemical screening and pharmacological analysis. For the separation and partitioning of ethanolic extract (500 g) into distilled water and ethyl acetate, an equal amount of both (500 mL of each) was used in a separating funnel with vigorous shaking. After the formation of two immiscible layers, they were separated by evaporation and lyophilization. The total amount of ethyl acetate extract was 126 g, and the total amount of aqueous fraction was 240 g, both collected separately. The yield of the extract was determined by calculating the ratio of the weight of the extract obtained to the weight of the plant material used, expressed as a percentage using the equation:

$$\text{Percentage Yield} (\%) = (\text{Weight of Extract} / \text{Weight of plant}) \times 100$$

### 2.2. Layout of experiments and calculation of doses

Stock solutions of *C. bonplandianus* leaves extract, aqueous fraction, and standard drug (Indomethacin, Sigma Aldrich) were prepared in 0.9 % normal saline. The *C. bonplandianus* leaves ethanol extract (CBEE) and aqueous fraction (CBAF) and standard drug were freshly prepared and administered orally according to the rat's body weight. The doses of CBEE and CBAF in concentrations of 125 mg.kg$^{-1}$, 250 mg.kg$^{-1}$, and 500 mg.kg$^{-1}$ were chosen based on the previous study (Dutta et al., 2018) in order to assess their effect on Freund Complete Adjuvant (FCA) induced arthritis, while standard drug was administered at 10 mg.kg$^{-1}$. The rats in the control group were given normal saline (0.9 %), while the rats in the positive control group were given FCA. Further experimental design and timeline is given in Fig. 1.

### 2.3. Experimental animal models and induction of arthritis

All the protocols for animal model study design were approved (ORIC/LCWU/379) by the Research Ethics Institutional Review Board of Lahore College for Women University, Lahore, Pakistan.

To evaluate the anti-arthritic activity, 6 – 8 weeks old male Sprague-Dawley rats weighing 210 – 250 g were employed. All model animals were obtained from University of Veterinary and Animal Sciences in Lahore, Punjab, Pakistan. Rats were housed in polypropylene cages with rice husks as bedding and constant access to free water and normal pellet food. All other parameters remained constant, such as the relative humidity levels of 60 to 70 percent, the temperature of 28 °C, and the 12-hour cycles of darkness and light. Prior to beginning pharmaceutical activity, the animals were left to spend a week adjusting to their new surroundings (Kyei et al., 2012).

The arthritis was induced in 8 groups (n = 5 rats per group) using a 0.1 mL injection of FCA. The FCA solution was made by adding heat-killed *Mycobacterium tuberculosis* (1 mg/ml) to solution A, comprised of mannide monooleate (0.15 mL) and paraffin oil (0.85 mL). The FCA solution was administered into the sub-plantar surface of the left footpad of all eight groups of animals except the vehicle control group.

### 2.4. Arthritic score using macroscopic arthritic scoring technique

To evaluate severity and incidence of inducted arthritis, arthroscopy and microscopic scoring was utilized. The morphology and characteristic features of animals were assessed by physical examination of ipsilateral and contralateral paws and as per physical characteristics, a scoring criterion was set (Score = 0 to normal Paw, 1 = minimal, 2 = mild, 3 = moderate, 4 = severs swelling and redness) as described by (Kumar et al., 2013). In addition, if the contralateral paw was also involved it was scored as 5.

### 2.5. Evaluation of physical parameters after therapeutic effects of CBEE and CBAF on arthritis

The hind paw diameter of the rats injected with FCA was measured using a vernier caliper at regular intervals of 0, 5-, 10-, 15-, and 20-days post-injection. Additionally, the body weight and paw thickness of the animals were also recorded on the same days, as per the method described by (Kumar et al., 2013).

### 2.6. Evaluation of biochemical and hematological parameter after therapeutic effects of CBEE and CBAF on arthritis

The rats were euthanized using ketamine and xylazine anesthesia at the end of the trial. The blood was collected through cardiac puncture. Hematological factors such as total leukocyte count, red blood cells, hemoglobin content, and platelet count were measured using Swelab alva Plus hematology analyzer. Erythrocyte sedimentation rate was determined using CNWTC Med, China, Model ESR Fast Detector-OEM.
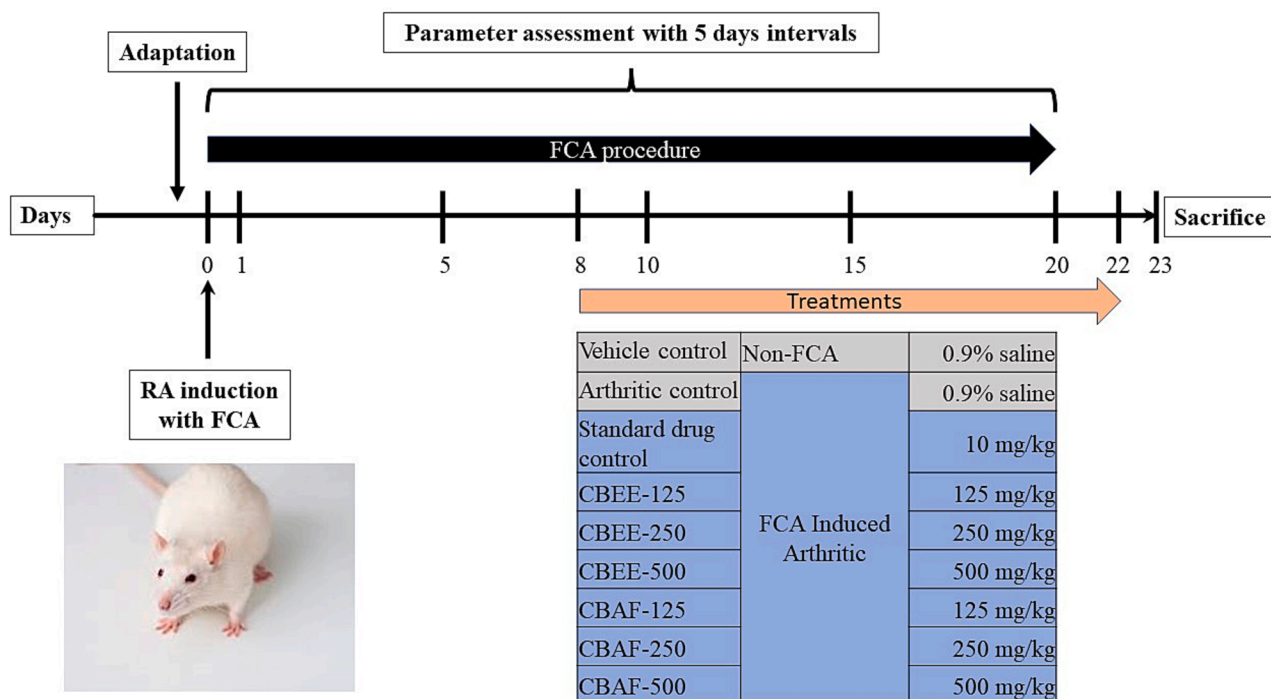
**Fig. 1.** Experimental design, time frame and dosing concentrations for the treatment of arthritis induced inflammation.

In addition, biochemical factors were also measured, to check effects of CBEE and CBAF treatments on liver and kidney function, using commercial kits and a fully automated biochemistry analyzer and as per instructions of the kit manufacturers.

### 2.7. Determination of mRNA expression levels after CBEE and CBAF treatment

The total RNA was extracted and purified according to the Magen Kit manufacturer's protocols. To analyze the inflammation patterns in rat groups treated with CBEE and CBAF treatments, IL-6, IL-1β, and TNF-α genes expressions were evaluated using RT-qPCR. The percentage of purity and yield were then analyzed by nanodrop. The cDNA was then synthesized with reverse transcriptase enzyme, as per instructions of kit manufacturer (Zokeyo China). The Real-time PCR reaction contained SYBR Green (2x) PCR master mix, ROX (internal dye from Thermo Scientific, America), gene-specific primers (0.2 μM each), and nuclease-free water. The details of gene specific primer is given in Table 1. The mixture was then placed in a qPCR thermal cycler (Bio-red) and underwent 45 cycles of denaturation (95 °C), annealing (60 °C), and termination (72 °C) (Shabbir et al., 2016).

### 2.8. Histopathological examination of rat joints

After sacrifice of the rats, ankles were then placed in a solution of 10 % formalin and PBS for preservation. The ankles of all animals were taken up to a level of the medial and lateral malleoli. In addition, paws were preserved after collection in formalin 10 % followed by histopathological evaluation as per instructions mentioned in (Shabbir et al.,

2016). A histopathologist, unaware of the treatment groups, analyzed parameters of inflammation, pannus development, and bone resorption.

### 2.9. Mass spectrometry (GC–MS) analysis of CBEE and CBAF

An Agilent (7890B) gas chromatograph having an inert mass selective detector (5977B) and DB-5MS GC column, having a length of 30 m, internal diameter of 0.25 mm, and film thickness of 0.25 μm, was used for GC–MS analysis of CBEE and CBAF. A split less mode was used to inject 2 μL of each sample, while injector had the temperature of 250 °C and an interface temperature of 280 °C. In addition, the oven temperature was automated to start from 100 °C for 0.5 min, followed by a ramp of 20 °C per minute until it reached 340 °C. For electron spray ionization, helium carrier gas was incorporated at full-scan mode at –70 eV. The complete cycle for each sample was about 30 min.

### 2.10. Molecular docking of CBEE and CBAF compounds

All compounds were first sketched using Molecular Operating Environment (MOE 2019.01) and for additional preparations. The MOE software was used to perform all computational tasks, including ligand and protein interactions, molecular docking, rescoring, analysis, and 2D intermolecular pattern determination (Gagné-Boulet et al., 2021).

### 2.11. Preparation of compounds as ligands for molecular docking

All compounds isolated from GC–MS of CBEE were first constructed using MOE's Builder module. These structures were further prepared using the Ligand Preparation module, amplified to assign the correct charges, optimized geometry, and minimized structures using the MMFF94x force field and a 0.1 kcal/mol of energy convergence gradient criteria (Uchikoga et al., 2013).

### 2.12. Preparation of crystal structure

An in-depth literature was searched to find the most potential targets for RA and IL-1β, IL-6 and TNF-α factors. For in silico studies, 3D

**Table 1**
The sequences of the forward and reverse primers used for the TNF-α, IL-6 and IL-1β genes.

| Gene | Forward | Reverse |
|------|---------|---------|
| TNF-α | 5′-CCTCTTCTCATTCCTGCTCGT-3′ | 5′-TGAGATCCATGCCATTGGCC-3′ |
| IL-6 | 5′-AGACTTCCAGCCAGTGCCC-3′ | 5′-CTGACAGTGCATCATCGC TG-3′ |
| IL-1β | 5′-GCTGTCCAGATGAGAGCATC-3′ | 5′-GTCAGACAGCACGAGGCATT-3′ |

structures of proteins, including PDB: 1ITB for IL-1β, PDB: 5FUC for IL-6, and PDB: 2AZ5 for TNF-α, were obtained from the RCSB protein data bank (PDB). The crystal forms of each factor were critically examined for missing residues, and were then subjected to MOE's structure preparation module, which was specifically designed to correct and impose appropriate charges on the protein along with geometry optimization. These structures were minimized with AMBER10: EHT forcefield and saved for docking.

### 2.13. Molecular docking and scoring

The IL-1β was complexed with its receptor IL-1R. Its binding site was dissected into two subsites of fifteen residues, designated A and B (PDB: 1ITB). To identify the potential binding site, compounds were docked using a blind-docking protocol with default parameters. A critical analysis of clustering composite conformations by generating 100 conformations of each compound was performed, which were further evaluated by score-based ranking (Sardar et al., 2022).

For the binding site of IL-6 the interface residues were targeted to inhibit the IL-6/IL-6R using induced fit model, and Triangle Matcher algorithm with London dG and GBIV/WSA dG as re-scoring function were applied (Mustafa et al., 2021). Collectively, 30 conformations for docking simulation were obtained and the best-scored conformations were designated for comprehensive interaction examination.

Before docking of TNF-α, the redocking of co-crystallized ligand was validated to assess the consistency of the docking protocol used, while different algorithms and scoring functions were applied to replicate its orientation by root mean square deviation (RMSD) (Zia et al., 2020). A total of 30 conformations were established and the best scored conformations were selected for a comprehensive analysis of the interaction pattern.

### 2.14. Statistical analysis

GraphPad Prism 8.0.2 (2 6 3) was employed for data analysis. One-way ANOVA was applied along with Dennett's post Hoc test to determine if any group's mean value was different from the other. Values were shown as mean ± SEM. The value of $p \leq 0.05$ was considered statistically significant.

## 3. Results

FCA induced arthritis produced significant signs and symptoms of inflammation in hind paw at 2nd day of arthritic induction in all animal models, as well as the macroscopic arthritic scores were also significantly higher in the rat groups (all) as compared with the vehicle control group ($p < 0.001$). However, no significant difference was seen in all

FCA induced rats of all groups compared with each other (Fig. 2).

### 3.1. Therapeutic effects of CBEE and CBAF on physical parameters

For the assessment of therapeutic effects of CBEE and CBAF, nine groups of rats (n = 5 per group) were utilized. Group one served as the vehicle control group (no arthritis and no treatment), group two as the arthritic control group (disease control rats with no treatment), and group three as the standard drug group (arthritic rats treated with indomethacin). The remaining six groups were assigned to receive CBEE and CBAF treatments at doses of 125 mg/kg, 250 mg/kg, and 500 mg/kg, respectively. The body weight (in grams) of the rats in the CBEE and CBAF treated groups at the prescribed doses was measured at time intervals of 0, 5, 10, 15, and 20 days after treatment. The results revealed a significant and consistent decrease in body weight in the arthritic control group ($p < 0.05$) compared to the vehicle control group (Fig. 3A and B). Additionally, a significant difference was observed in Dunnett's post-hoc statistical analysis in rat body weight at 5, 10, 15, and 20 days between the arthritic control group and the standard drug group ($p < 0.05$), as well as between the arthritic control group and the CBEE treatment groups at doses of 125 mg/kg, 250 mg/kg, and 500 mg/kg (Fig. 3A, $p < 0.05$ for all CBEE treatments), and the CBAF treatment groups at doses of 125 mg/kg, 250 mg/kg, and 500 mg/kg (Fig. 3B, $p < 0.05$ for all CBAF treatments). In contrast, the body weight of the vehicle control group showed no significant difference when compared to the seven treatment groups, including Indomethacin, and the six groups receiving CBEE and CBAF treatments at doses of 125 mg/kg, 250 mg/kg, and 500 mg/kg.

Paw thickness (in mm) was assessed following CBEE and CBAF treatments (Fig. 3C and D, respectively) at doses of 125 mg/kg, 250 mg/kg, and 500 mg/kg on days 0, 5, 10, 15, and 20. Paw thickness significantly increased in the arthritic control group compared to the vehicle control group ($p < 0.05$), as well as in the arthritic control group compared to the CBEE doses (Fig. 3C) of 125 mg/kg ($p < 0.05$), 250 mg/kg ($p < 0.05$), and 500 mg/kg ($p < 0.05$), and the CBAF doses (Fig. 3D) of 125 mg/kg ($p < 0.05$), 250 mg/kg ($p < 0.05$), and 500 mg/kg ($p < 0.05$). At day 0, no significant differences were observed between the vehicle control group versus the arthritic control group or between the arthritic control group versus any of the four treatment groups ($p > 0.05$).

Furthermore, hind paw images were taken on day 23 of the experiment (Fig. 4). According to the analysis, the vehicle control group displayed a thin and normal paw with no physical swelling or redness, while the arthritic control group exhibited physical swelling and redness by day 23. The standard drug control group on day 23 showed less physical swelling and redness compared to the vehicle control group. The CBEE treatments on day 23 post-treatment displayed less physical
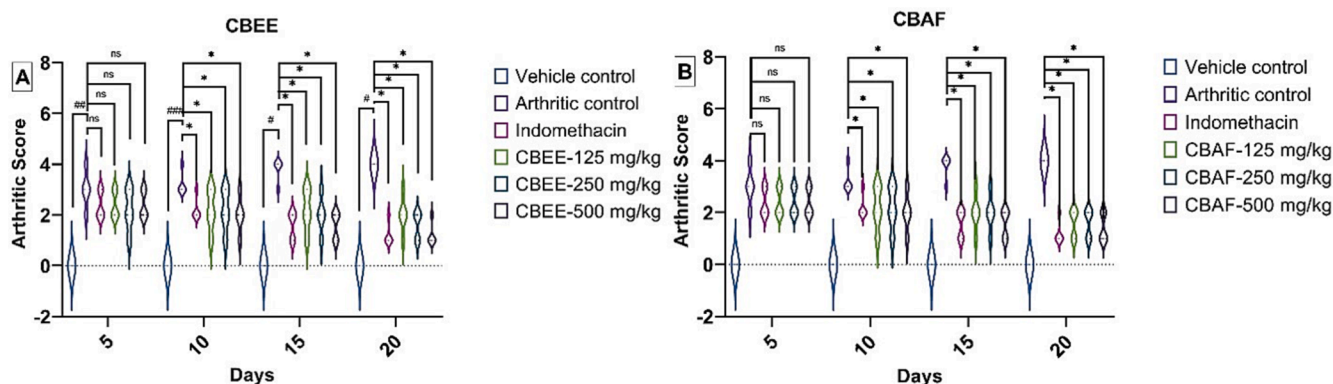


**Fig. 2.** Arthritic scoring of CBEE and CBAF (A and B respectively, n = 5 per group) treatments at 5, 10, 15, and 20th days. Results are given as mean ± SEM. Where # is significance (p < 0.05) between vehicle control vs arthritic control and * shows significance as Dunnett's post-hoc test between arthritic control vs treatment (p < 0.05).
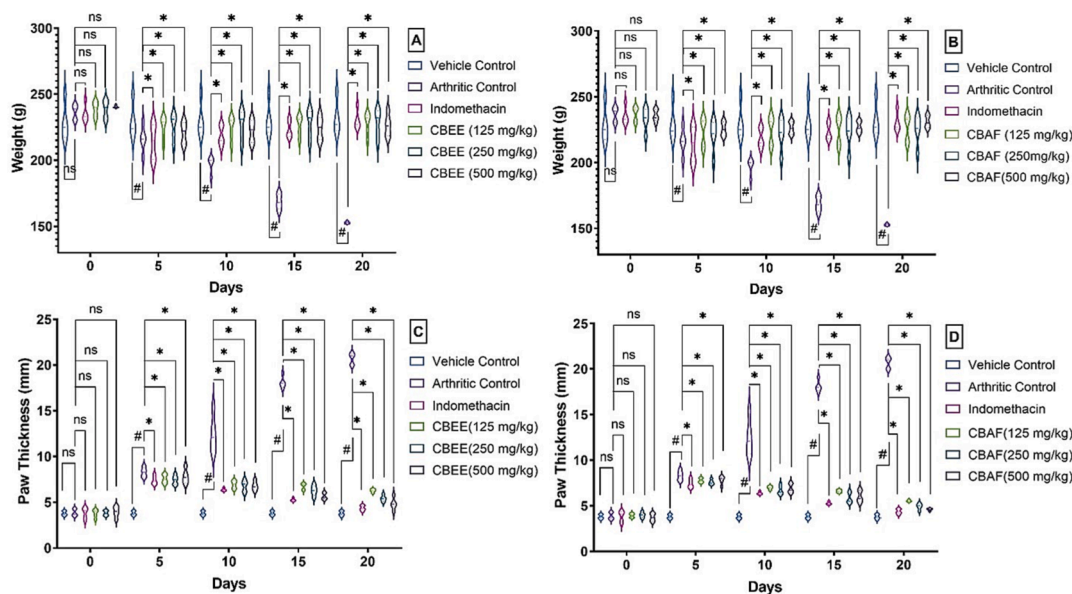
**Fig. 3.** Effects of CBEE at 125, 250 and 500 mg/kg and CBAF at 125, 250 and 500 mg/kg on the body weight of rats (A and B respectively, n = 5 per group), and on the paw thickness (C and D). Results are given as mean ± SEM. Where # is significance (p < 0.05) between vehicle control vs arthritic control and * significance as Dunnett's post-hoc test between arthritic control vs treatment (p < 0.05).



**Fig. 4.** FCA injected hind paws of rats treated with CBEE and CBAF at 125,250,500 mg/kg doses, whereas the images were taken on 23rd day post treatment. VC = Vehicle Control, AC = Arthritic Control, CBEE = C. bonplandianus ethanolic extract (125, 250, 500 mg/kg, b.w), CBAF = (C. bonplandianus aqueous fraction (125,250,500 mg/kg, b.w).

swelling and redness at a dose of 500 mg/kg; however, physical swelling and redness were still observed at doses of 125 mg/kg and 250 mg/kg. Additionally, the CBAF treatments on day 23 after treatment at 125 mg/kg, 250 mg/kg, and 500 mg/kg also showed physical swelling and redness in all treatment groups.

### 3.2. Therapeutic effects of CBEE and CBAF on biochemical and hematological parameters

The therapeutic effects of CBEE and CBAF on biochemical and hematological parameters were assessed on day 23 after treatment with doses of 125 mg/kg, 250 mg/kg, and 500 mg/kg for both treatments. However, no significant changes in serum concentrations of AST, ALT, urea, and creatinine (Fig. 5A – D) were observed when comparing the arthritic control group to the vehicle control group (p > 0.05). Additionally, there were no significant differences in the concentrations of these biochemical parameters when comparing the arthritic group to the standard drug treatment group (p > 0.05). Among the treatment groups, the arthritic group showed significant changes in AST levels in the CBAF treatments at 250 mg/kg (p < 0.01) and 500 mg/kg (p < 0.001) when
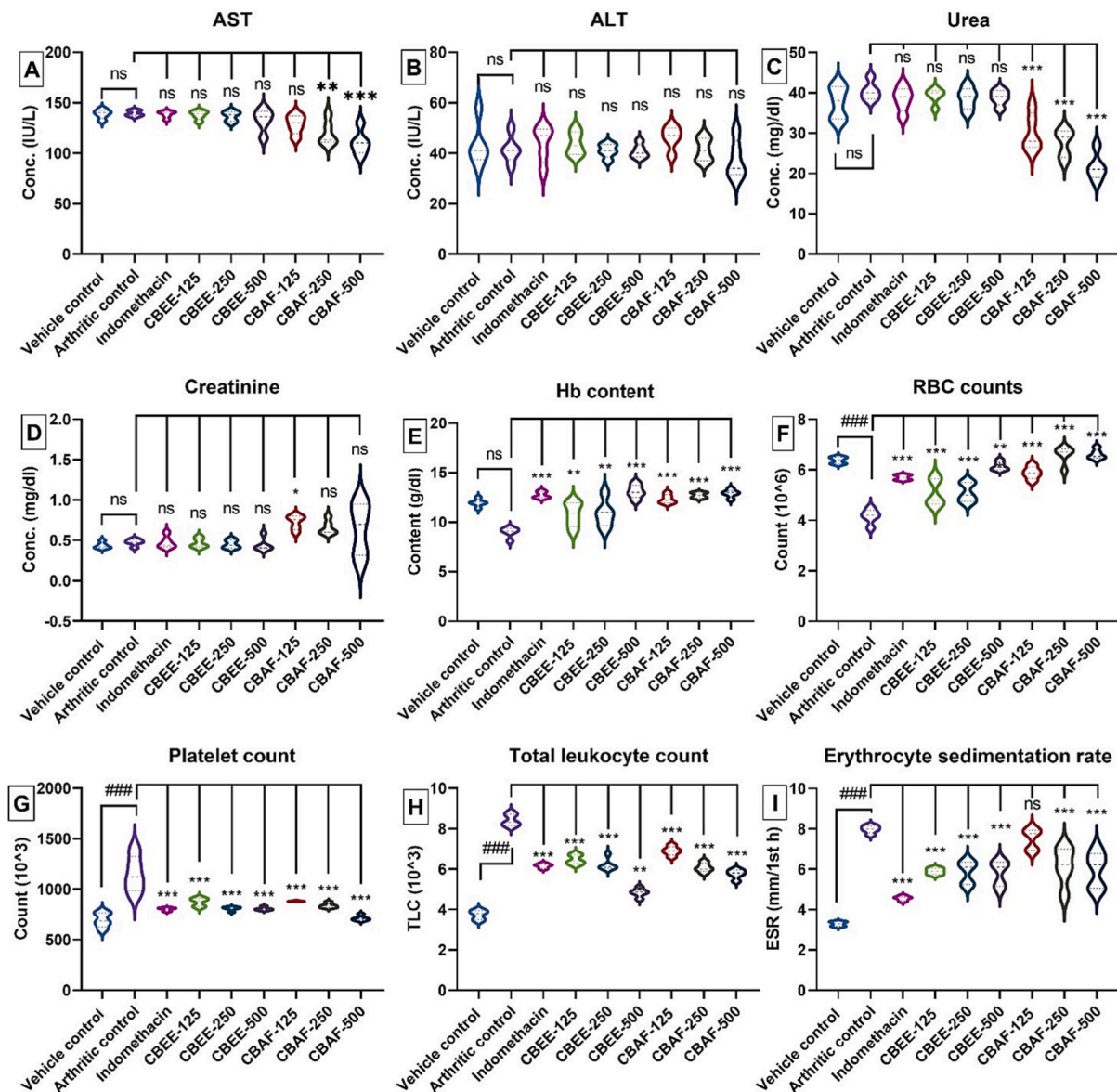
**Fig. 5.** Effects of different doses of CBEE and CBAF on biochemical parameters [AST (A), ALT (B), urea (C), and creatinine (D)] and hematological parameters [hemoglobin content (E), red blood cell count (F), platelets count (G) total leukocyte count (H), and ESR (I)]. The sign ns indicates non-significant, # indicates significant difference in biochemical parameters between vehicle control and arthritic control and * indicates significance and $p < 0.05$ (*), $p < 0.01$ (**), $p < 0.001$ (***). All values are given as mean $\pm$ SEM.

compared to the arthritic group. Urea levels also differed significantly in CBAF treatments at doses of 125 mg/kg, 250 mg/kg, and 500 mg/kg ($p < 0.001$ for all CBAF treatments) when compared to the arthritic group.

Hematological parameters, including hemoglobin content (g/dL, Fig. 5E), red blood cell count (CFUs, Fig. 5F), platelet count (CFUs, Fig. 5G), total leukocyte count (CFUs, Fig. 5H), and ESR (mm/1st hour, Fig. 5I), were also measured on the 23rd day after treatments with CBEE and CBAF at respective doses of 125, 250, and 500 mg/kg. The concentrations of all five hematological parameters in the vehicle control group differed significantly compared to the arthritic control group ($p < 0.001$). Furthermore, significant differences were also observed in the concentrations of all hematological parameters when comparing the arthritic control group to 1) the standard drug group ($p < 0.001$), 2) the CBEE treatments at doses of 125 mg/kg, 250 mg/kg, and 500 mg/kg (for all CBEE treatments, $p < 0.01$), and 3) the CBAF treatments at doses of 125 mg/kg, 250 mg/kg, and 500 mg/kg (for all CBAF treatments, $p < 0.01$).

### 3.3. Effects of CBEE and CBAF treatments on gene expression

The gene expression profiles of three inflammatory cytokine genes, namely IL-6, IL-1β, and TNF-α, were assessed in all groups, including the vehicle control, arthritic control, standard drug treatment, and treatments with doses of 125 mg/kg, 250 mg/kg, and 500 mg/kg for both CBEE and CBAF (Fig. 6). A significant difference in the expression levels (fold change) of IL-1β, IL-6, and TNF-α genes was observed between the vehicle control and arthritic control groups ($p < 0.001$). Furthermore, there was a significant difference in the expression levels (fold change) of IL-1β, IL-6, and TNF-α genes between the arthritic control group and the treatment groups, including standard drug and doses of 125 mg/kg, 250 mg/kg, and 500 mg/kg for both CBEE and CBAF treatments ($p < 0.001$), except for the comparison between the arthritic control group and the CBEE 125 mg/kg dose treatment, which was non-significant ($p > 0.05$).
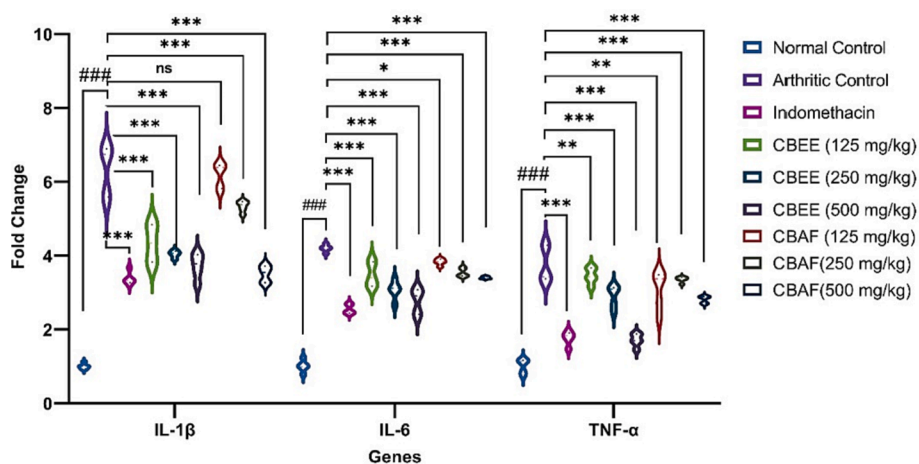
**Fig. 6.** Effects of different doses of CBEE and CBAF on gene expression in fold change of IL-1β, IL-6, and TNF-α. Results are displayed as mean ± SEM and n = 5 per group. The significance ### = p < 0.001 between vehicle control group vs arthritic control group, for arthritic control group vs treatments groups significance is given as ns = non-significant, * = p < 0.05, ** = p < 0.01, and *** = p < 0.001.

### 3.4. Mass spectrometric analysis of the CBEE and CBAF

The CBEE was chemically profiled using gas chromatography-mass spectrometry (GC–MS) for organic phytochemicals. The mass spectrometric analysis of CBEE and CBAF revealed 48 compounds (Table 2) and 15 compounds (Table 3), respectively, which were confirmed based on their peak area, molecular weight (MW), retention time, and molecular formula.

### 3.5. Computational biology and molecular modelling

To discover the inhibitory role of total 60 compounds of both CBEE and CBAF, observed in GC–MS, against IL-1β, IL-6 and TNF-α, computational study was utilized. Among 60 compounds, the top scored compounds and their interaction pattern with the respective protein are discussed below.

### 3.6. Inter-molecular interaction patterns and binding modes of IL-1β

Upon investigation the interface of IL-1β and IL-1R displayed two possible binding sites of fifteen residues, site A consisting of residues 11, 13–15, 20–22, 27, 29–36, 38, 126–131, 147, 149 while site B consist of 1–4, 6, 46, 48, 51, 53–54,56, 92–94,103, 105–106, 108, 109, 150 and 152. Application of a blind docking protocol resulted in the identification of a major cluster of ligand conformations that dwells in site B. Due to the occupancy of denser clusters at site B, it was concluded as promising target sites for our compounds. The binding mode of the most potent inhibiting compounds suggested Hentriacontane from CBAF as most effective with the binding energy of −8.23 kcal/mol. Other compounds dock scores are shown in Table 4. The results depicting all the top scored selected compounds in the proximity of site B pocket of protein interacting with the crucial residues are shown in 2D interaction pattern in Fig. 6. Among these Palmitoyl Amide formed hydrogen bond with Ser43 as a side chain donor shown in Fig. 7.

### 3.7. Inter-molecular interaction patterns and binding modes of IL-6

To obstruct the interaction of IL-6/IL-6R, the contacting interface residues were targeted for the docking simulation. The interface residues are composed of the following residues i.e., Chain A: 30, 51, 74, 75, 76 168, 172, 179, 182, 183 Chain D: 163, 166, 190, 228, 229, 277, 278, 28. A total of 50 conformations were produced while applying induced fit, Triangle Matcher algorithm (London dG and GBIV/WSA dG as rescoring function) and keeping other parameters as default. The binding of

Hentriacontane from aqueous extract to be most effective with the binding energy of −8.18 kcal/mol as shown in Table 4. All the highest scored compounds were found to be in interface proximity of IL-6/IL-6R having major interactions with 30A, 51A, 168A, 172A, 182A, 190D, 278D and 281D. Palmitoyl amide formed three hydrogen bonds with Thr248, Arg274 and Glu283 while one hydrogen bond was observed in ligand–protein complex of Gamma tocopherol and Phytol with Val251 and Arg233, respectively in Fig. 7. All selected compounds' 2D interaction pattern can be visualized in Fig. 8 and their dock scores are mentioned in Table 3.

### 3.8. Inter-molecular interaction patterns and binding modes of TNF-α

To assess the coherence of the MOE software, redocking of the co-crystallized ligand in the TNF-α protein was performed. Various algorithms were tested and based on the RMSD (Root Mean Square Deviation) value of 0.28 Å (which was less than 3 Å), the induced fit and ASE algorithms, along with the GBIV/WSA dG Triangle Matcher algorithm as rescoring functions, yielded valuable results.

Among all the GC–MS compounds, Palmitoyl amide exhibited the highest binding energy (8.81 kcal/mol) and formed hydrogen bonds with two side chains, namely Gln61 and Tyr151. Stigmasterol and Hexadecenoic acid from the aqueous fraction each formed a single hydrogen bond with Tyr119 and Tyr151, respectively. In contrast, DL-proline and Beta-tocopherol displayed hydrophobic interactions involving their benzene rings with Leu57 and Gly121, respectively. All these compounds were found within the binding cavity of TNF-α, as illustrated in Fig. 9. The dock score and 2D interaction patterns for all compounds are presented in Table 3 and Fig. 9.

### 3.9. Histopathological examination of ankle joints

Histopathological analysis of rat paws injected with FCA was conducted. Treatment with both CBEE and CBAF significantly reduced inflammation in a dose-dependent manner when compared to the arthritic control group. Additionally, the standard drug group treated with Indomethacin exhibited a reduction in inflammation compared to the arthritic control group (Fig. 10).

Histological examination of the sections revealed that the arthritic control group displayed severe acute and chronic inflammatory reactions in periarticular tissue. Furthermore, disease effects in the form of inflammation and pannus formation were also observed. In the Indomethacin-treated group, the treatment led to a decrease in inflammation and an increase in joint space. CBEE treatment at 125 mg/kg

**Table 2**
Mass spectrometric (GCMS) analysis of CBEE for phytochemical profile.

| Sr. No. | Peak No. | RT (min) | Compound Name | Mol. Formula | Mol. Weight |
|---|---|---|---|---|---|
| 1 | 3 | 1.401 | Xylitol | $C_5H_{12}O_5$ | 152.15 |
| 2 | 4 | 1.456 | Erythritol | $C_4H_{10}O_4$ | 122.12 |
| 3 | 6 | 1.635 | D1-Threitol | $C_4H_{10}O_4$ | 122.2 |
| 4 | 22 | 3.523 | Betaine | $C_5H_{11}NO_2$ | 117.15 |
| 5 | 22 | 3.523 | 1-Methylpiperazine | $C_5H_{12}N_2$ | 100.16 |
| 6 | 23 | 3.573 | Naphthalene, 1,2-dihydro-4,6,8-trimethyl- | $C_{13}H_{16}$ | 172.27 |
| 7 | 24 | 3.768 | Nicotine | $C_{10}H_{14}N_2$ | 162.23 |
| 8 | 25 | 3.833 | Alpha.- Pyrrolidone, 5-[3-hydroxybutyl] | $C_8H_{15}NO_2$ | 157.21 |
| 9 | 26 | 3.934 | DL-Proline, 5- oxo, methyl ester | $C_6H_9NO_3$ | 143.14 |
| 10 | 27 | 4.018 | 1-Pyrrolid-2-one | $C_4H_7NO$ | 85.1 |
| 11 | 27 | 4.018 | Aziridine | $C_2H_5N$ | 43.07 |
| 12 | 28 | 4.154 | 2H-Azepin-2- one, 3-(dimethylamino) hexahydro- | $C_8H_{16}N_2O$ | 156.23 |
| 13 | 29 | 4.248 | Azetidine | $C_3H_7N$ | 57.09 |
| 14 | 30 | 4.365 | 6-Azathymine | $C_4H_5N_3O_2$ | 127.1 |
| 15 | 33 | 4.54 | Theobromine | $C_7H_8N_4O_2$ | 180.16 |
| 16 | 38 | 5.16 | Sedoheptulosan | $C_7H_{12}O_6$ | 192.17 |
| 17 | 41 | 5.358 | 4-Furfurylidene- 5-ox-2-thiooxoi… | | |
| 18 | 42 | 5.609 | Fumaric acid | $C_4H_4O_4$ | 116.07 |
| 19 | 46 | 5.944 | Loliolide | $C_{11}H_{16}O_3$ | 196.24 |
| 20 | 47 | 6.074 | Orcinol | $C_7H_8O_2$ | 124.14 |
| 21 | 47 | 6.074 | Piperidine | $C_5H_{11}N$ | 85.15 |
| 22 | 48 | 6.141 | Neophytadiene | $C_{20}H_{38}$ | 278.5 |
| 23 | 49 | 6.272 | Carvone | $C_{10}H_{14}O$ | 150.22 |
| 24 | 50 | 6.324 | Hydrazine | $N_2H_4$ | 32.05 |
| 25 | 51 | 6.375 | Oxazolidine | $C_3H_7NO$ | 73.09 |
| 26 | 52 | 6.375 | Dimethoate | $C_5H_{12}NO_3PS_2$ | 229.3 |
| 27 | 61 | 7.594 | Phytol | $C_{20}H_{40}O$ | 296.5 |
| 28 | 68 | 8.294 | Thymol | $C_{10}H_{14}O$ | 150.22 |
| 29 | 69 | 8.359 | Inositol | $C_6H_{12}O_6$ | 180.16 |
| 30 | 79 | 9.402 | Palmitic acid | $C_{16}H_{32}O_2$ | 256.42 |
| 31 | 83 | 9.717 | Flexibilide | $C_{20}H_{30}O_4$ | 334.4 |
| 32 | 90 | 10.45 | Palmitoyl-ethanol amide | $C_{18}H_{37}NO_2$ | 299.5 |
| 33 | 103 | 11.64 | Gamma- tocopherol | $C_{28}H_{48}O_2$ | 416.7 |
| 34 | 104 | 11.8 | Tamoxifen | $C_{26}H_{29}NO$ | 371.5 |
| 35 | 106 | 12.09 | Vitamin E | $C_{29}H_{50}O_2$ | 430.7 |
| 36 | 107 | 12.15 | Trans- Geranylgeraniol | $C_{20}H_{34}O$ | 290.5 |
| 37 | 109 | 12.44 | Scoparone | $C_{11}H_{10}O_4$ | 206.19 |
| 38 | 110 | 12.55 | Pinoresinol | $C_{20}H_{22}O_6$ | 358.4 |
| 39 | 111 | 12.77 | Campesterol | $C_{28}H_{48}O$ | 400.7 |
| 40 | 112 | 12.94 | Stigmasterol | $C_{29}H_{48}O$ | 412.7 |
| 41 | 115 | 13.44 | Beta-Sitosterol | $C_{29}H_{50}O$ | 414.7 |
| 42 | 116 | 13.52 | Stigmasta − 5,24(28)-diene-3-ol | | |
| 43 | 116 | 13.52 | Androst-5,15- diene-30 l acetate | $C_{21}H_{30}O_2$ | 314.5 |
| 44 | 117 | 13.79 | Beta- Amyrin | $C_{30}H_{50}O$ | 426.7 |
| 45 | 119 | 14.19 | Alpha-Amyrin | $C_{30}H_{50}O$ | 426.7 |
| 46 | 123 | 14.98 | Lupeol | $C_{30}H_{50}O$ | 426.7 |
| 47 | 123 | 14.98 | Lanosterol | $C_{30}H_{50}O$ | 426.7 |
| 48 | 125 | 17.2 | Syringaresinol | $C_{22}H_{26}O_8$ | 418.4 |

**Table 3**
Mass spectrometric (GCMS) analysis of CBAF for phytochemical profile.

| Sr. No. | Peak No. | RT (min) | Compound Name | Mol. Formula | Mol. Weight |
|---|---|---|---|---|---|
| 1 | 1 | 3.982 | Beta-Gurjunene | $C_{15}H_{24}$ | 204.35 |
| 2 | 2 | 4.177 | Phenol, 2,4-bis(1,1-dimethylethyl) | $C_{17}H_{30}OSi$ | 278.5 |
| 3 | 3 | 4.847 | Hydroxyl-beta-demascone | $C_{13}H_{20}O_2$ | 208.3 |
| 4 | 3 | 4.847 | Farnisol | $C_{15}H_{26}O$ | 222.37 |
| 5 | 3 | 4.847 | Dinocap I, II, III | | |
| 6 | 5 | 5.361 | Heneicosane | $C_{21}H_{44}$ | 296.6 |
| 7 | 11 | 5.85 | Eicosane | $C_{20}H_{42}$ | 282.5 |
| 8 | 19 | 6.429 | Silane, diphenyldi(non-5-yn- 3-yl) | $C_{48}H_{32}Si$ | 636.8 |
| 9 | 21 | 6.545 | Hentriacontane | $C_{31}H_{64}$ | 436.8 |
| 10 | 22 | 6.609 | Palmitic acid | $C_{16}H_{32}O_2$ | 256.42 |
| 11 | 29 | 7.015 | Pentacosane | $C_{25}H_{52}$ | 352.7 |
| 12 | 32 | 7.504 | 11-Methtlpentacosane | | |
| 13 | 80 | 15.9 | Cinnamoyl Ferrocene | | |
| 14 | 81 | 16.23 | Benzenepropanoic acid | | |
| 15 | 81 | 16.23 | Beta-Tocopherol | $C_{28}H_{48}O_2$ | 416.7 |

**Table 4**
Dock Score of the top selected compounds against IL-1β, IL-6 and TNF-α.

| S.No. | Compounds | Dock Score (kcal/mol) | | |
|---|---|---|---|---|
| | | IL-1β | IL-6 | TNF-α |
| 1. | Hentriacontane | −8.23 | −8.18 | −7.85 |
| 2. | Pentacosane | −7.49 | −7.76 | N/A |
| 3. | Heneicosane | −7.08 | −7.88 | N/A |
| 4. | Hexadecenoic acid | −7.03 | N/A | −7.12 |
| 5. | Beta-tocopherol | N/A | −7.16 | −7.08 |
| 6. | Palmitoylethanol Amide | −7.24 | −6.40 | −8.81 |
| 7. | Gamma-tocopherol | N/A | −6.31 | −7.66 |
| 8. | DL-Proline | N/A | N/A | −7.10 |
| 9. | Neophytadiene | −7.76 | N/A | N/A |
| 10. | Phytol | N/A | −6.15 | N/A |
| 11. | Vitamin E | N/A | N/A | −7.63 |
| 12. | Stigmasterol | N/A | N/A | −7.48 |
| 13. | Beta-sitosterol | N/A | −6.39 | N/A |
| 14. | Syringaresinol | −7.36 | N/A | N/A |
| 15. | Beta-Amyrin | −6.63 | N/A | N/A |

resulted in a mild treatment effect on the joints; however, inflammation was still observed in this group of rats. CBEE treatment at 250 mg/kg showed the formation of fibro-inflammatory adhesions between bone and soft tissue. CBEE treatment at 500 mg/kg demonstrated effective results, with signs of inflammation healing.

CBAF treatment at 125 mg/kg showed improvement in joint space and the articular surface of the joint bones. In the CBAF-250 mg/kg group, inflammatory cells in the joint space were observed. The CBAF treatment at 500 mg/kg also displayed effective results, with signs of inflammation healing.

## 4. Discussion

The demand for medicines or dietary supplements from natural sources has increased exponentially, as they could potentially cure any disease with fewer side effects (Dutta & Chaudhuri, 2018). Several plants have been used as anti-inflammatory agents with significant effects compared to traditional anti-inflammatory drugs (Adebayo & Masoko, 2017; Uytan et al., 2021; Yasin et al., 2021). Among natural sources, *C. bonplandianus* has various therapeutic uses, including repellent of insects, antibacterial, antifungal, antioxidant, analgesic, nematocidal, coronary, hepatoprotective and wound healing (Dutta & Chaudhuri, 2018). Moreover, the leaves of *C. bonplandianus* were also used to treat skin diseases and conventionally used on external cuts and wounds (Rajakaruna et al., 2002). In this study, the therapeutic potential of the ethanolic extracts of leaves of *Croton bonplandianus* (CBEE) and aqueous fractions of leaves of *Croton bonplandianus* (CBAF) against the rheumatoid arthritis-induced inflammation was evaluated. In addition, the therapeutic effects were measured in terms of body weight, paw thickness, biochemical and hematological parameters, expression of inflammatory genes, and histopathological examination of animal models. Moreover, GC–MS analysis of CBEE and CBAF was also assessed, followed by molecular docking of identified compounds in GC–MS analysis against inflammatory gene factors.

The FCA-induced inflammatory arthritis models were used for this study, which are favored due to its resemblance to human arthritic
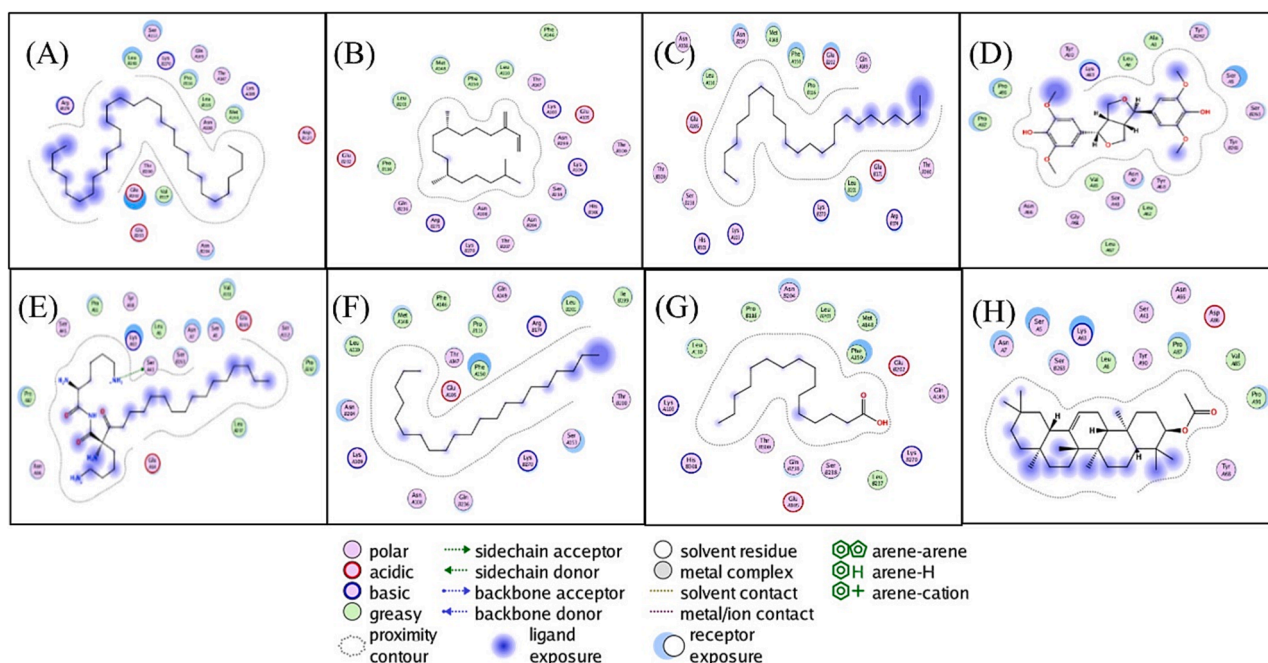
**Fig. 7.** Interaction pattern of (A) Hentriacontane (B) Neophytadiene (C) Pentacosane (D) Syringaresinol (E) Palmitoylethanol Amide (F) Heneicosane (G) Hexadecenoic acid (H) Beta-Amyrin.
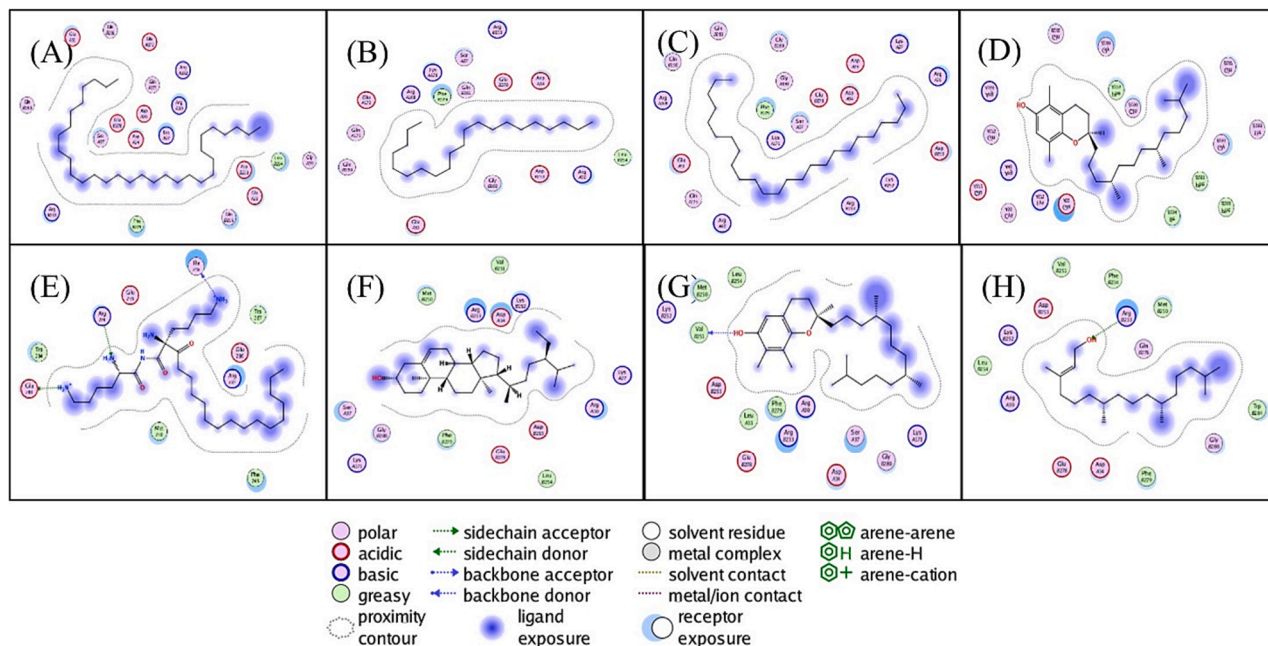


**Fig. 8.** Interaction pattern of (A) Hentriacontane (B) Heneicosane (C) Pentacosane (D) Beta-tocopherol (E) Palmitoylethanol Amide (F) Beta-sitosterol (G) Gamma tocopherol (H) Phytol.

diseases. It is characterized by synovial hyperplasia, vascular development, cartilage degradation, and bone erosion (Naz et al., 2020). Rheumatoid arthritis frequently causes weight loss and cachexia, which are caused by increased cytokine production, raising the resting metabolic rate and protein breakdown, as well as decreasing appetite. The arthritis in the FCA-induced model is measured macroscopically. Our recoded results of arthritic scores were decreasing in a time and dose-dependent manner in all CBEE and CBAF treatments compared to the arthritic group.

The treatments of CBEE and CBAF for 23 days at the doses of 125 mg.

kg$^{-1}$, 250 mg.kg$^{-1}$, and 500 mg.kg$^{-1}$ significantly reduced inflammatory effects of RA in rats of all treatments compared to the arthritic rats. The body weights remained relatively stable over time in the vehicle control group. In contrast, the body weights of rats in all treatment groups, including the standard drug group, showed an increase after treatment, and by day 23, the body weights in all treatment groups were relatively close to those in the vehicle control group. Additionally, the arthritic control group exhibited a significant and gradual loss in body weight over time (on days 5, 10, 15, and 20). Paw thickness, on the other hand, remained relatively consistent in all treatment groups when
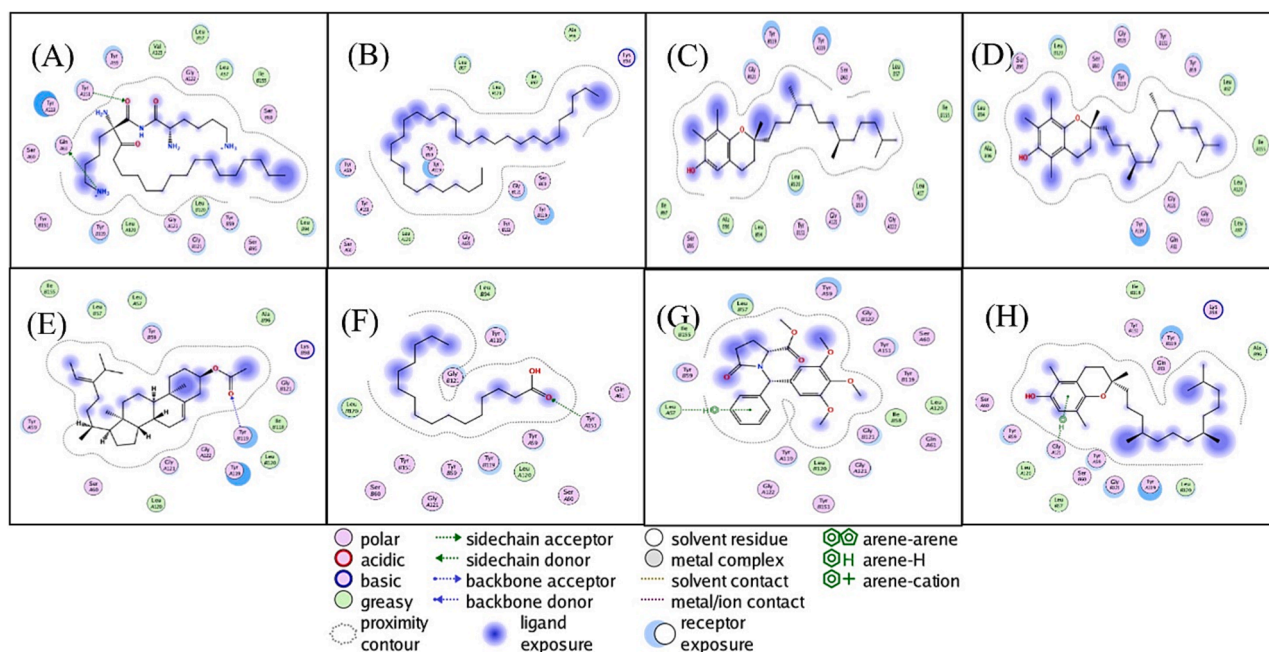
**Fig. 9.** Interaction pattern of (A) Palmitoylethanol Amide (B) Hentriacosane (C) Gamma-tocopherol (D) Vitamin E (E) Stigmasterol (F) Hexadecenoic acid (G) DL-Proline (H) Beta-tocopherol.

compared to the vehicle control group (p > 0.05). However, there were significant differences between the treatment groups and the arthritic control group, as well as between the arthritic control group and the vehicle control group (p < 0.05, Fig. 3C and D).

There is limited research on the treatment potential of ethanolic extracts from *C. bonplandianus* leaves against RA-induced inflammation. However, there have been reports of anti-inflammatory activity in methanolic extracts and aqueous extracts of *C. bonplandianus* leaves (Yasin et al., 2021). In addition, anti-inflammatory effects of oral extracts of *Jatropha gossypifolia* and *C. bonplandianus* with diclofenac sodium have also been reported, although the main anti-inflammatory components of *C. bonplandianus* are unknown (Ghosh, Biswas, et al., 2018). The anticancer activity of *C. bonplandianus* has also been described because of its antioxidant activity (Dutta et al., 2018; Ghosh, Biswas, et al., 2018). This cytotoxic effect of *C. bonplandianus* could scavenge ROS (reactive oxygen species), resulting in an anti-inflammatory effect (Yasin et al., 2021) which we also found on the hind paw images (Fig. 4).

The effect of the CBEE and CBAF treatments on biochemical and hematological parameters was also evaluated (Figs. 5 and 6). We observed that serum AST, ALT, urea, and creatinine concentrations were unaffected in the arthritic group compared to the vehicle control group (p > 0.05) except AST levels of CBAF treatments at 250 and 500 mg.kg$^{-1}$ and urea levels in all three treatment doses of CBAF compared to the arthritic control group (p < 0.01). Sengar and co-workers described significant increases in ALT, AST, and ALP enzymes in acute and sub-chronic models of inflammation, which were reduced to normal levels during EJS treatment at 400 mg.kg$^{-1}$. They linked this decrease in enzyme levels to either the enzymes not being released or the lysosomal membrane being stabilized (Sengar et al., 2015). A possible difference could be the concentration of the extract, as we also observed significant differences at higher doses.

The decrease in edema and arthritic score may be related to a decrease in prostaglandin release and neutrophil invasion (Babu et al., 2011). Secondary lesions arise in non-injected paws because of adjuvant activation of T cells. Immunosuppressants relieve arthritis by counteracting immune responses that are not suppressed by anti-inflammatory medications (Hasan et al., 2015). In our study, *Croton bonplandianus*

ethanol extract and aqueous fractions significantly decreased secondary lesions, thus implying an immunomodulatory effect in addition to anti-inflammatory properties and a reasonable reduction in cell arbitrated immunity (Talwar et al., 2011).

A decrease in Hb and RBC levels in arthritic control rats represents an anaemic condition caused by decreased erythropoietin levels, premature destruction of RBCs, bone marrow failure to respond to anemia, decreased plasma iron persuaded by IL-1, and abnormal iron loading in synovial tissue and the reticuloendothelial system (Uttra & Hasan, 2017). RBC and Hb levels were dramatically increased by the plant ethanol extract, aqueous fractions, and indomethacin. Furthermore, total leukocyte count is an important component of the host defensive system. The release of TNF-α and IL-1 in arthritis results in an increase in platelet and TLC counts (Uttra & Hasan, 2017). Reduction of TLC count and platelets (Fig. 5) in disease control rats and treatment groups displayed immunomodulation property of the plant extract (Ekambaram et al., 2010).

The elevated ESR count in the arthritic control group indicated the presence of more inflammatory proteins in circulation. However, the ethanol extract of the plant, the aqueous fraction, and the reference drug indomethacin significantly reduced ESR levels. It has been suggested that the injection of FCA causes T-cell stimulation, which in turn activates macrophages and monocytes, leading to increased lysosomal enzyme activity and the release of proinflammatory cytokines. The overexpression of pro-inflammatory cytokines contributes to the irreversible proliferation of synovial tissue, joint damage, tissue degradation, bone erosion, and programmed cell death in arthritic joints. (Mo et al., 2013).

Activated immune cells release several pro-inflammatory cytokines such as TNF- α, IL-1β and IL-6 which are often associated with rheumatoid arthritis pathogenesis. However, other cytokines such as IL-17 and VEGF also have their contribution in disease progression (Mahnashi et al., 2021). TNF-α and IL-1β have a pivotal role in rheumatoid arthritis by liberation of metalloproteases (for example collagenases, stromelysin) and prostaglandins from activated cells (such as macrophages, fibroblasts, and synovial dendritic cells). Although fibroblast-like synoviocytes also express IL-6, however most prominent feature of these cells is the production of huge amount of MMPs, prostaglandins
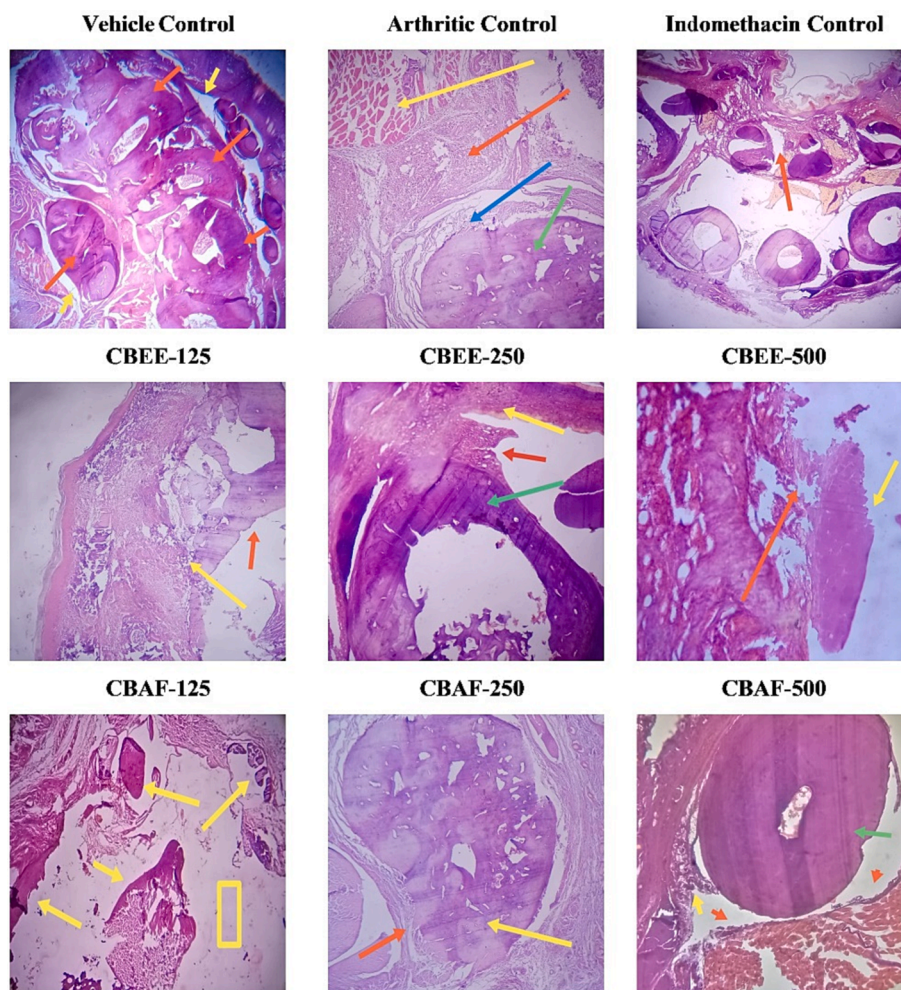
**Fig. 10.** Histopathological analysis of CBEE and CBEE at 23rd day. In Vehicle control, red arrow shows the bone, yellow arrow indicates the joint space. In disease group, yellow arrow shows muscle fibers, red arrow shows severe acute and chronic inflammatory reaction in peri articular tissue, blue arrow shows pannus and green arrow shows the bone. In Indomethacin group red arrow shows the joint space. In CBEE −125 mg/kg, red arrow indicates bone and yellow arrow indicates inflammation. In CBEE 250 mg/kg yellow arrow indicates periarticular soft tissue, red arrow adhesion of bone with soft tissue, green arrow shows the bone. In CBEE-500 mg/kg section red arrow indicates inflammatory infiltrate and yellow arrow shows the bone. In CBAF-125 mg/kg treatment section yellow arrow shows articular bone whereas yellow square shows the joint. In CBAF-250 red arrow shows inflammatory cells in joint space and yellow arrow shows the bone. In CBAF −500, red arrow shows the joint space and yellow arrow shows healing inflammation.

and leukotrienes (Aletaha & Smolen, 2018). Therefore, rheumatoid arthritis can be treated by subduing these inflammatory mediators resulting in improved quality of life (Moudgil & Venkatesha, 2022). Too fully understand the levels of specific genes, RT-qPCR was used. RT-qPCR technique achieves this through quantitative amplification of specific DNA or RNA segments, enabling precise measurement of the initial target molecule concentration in each sample. RT-qPCR results showed that administration of *C. bonplandianus* extracts notably reduced the expression of TNF-α, IL-1β and IL-6 which expresses its anti-inflammatory and anti-arthritic potential. TNF-α stimulates energy utilization by increasing lipolysis and protein catabolism and decreasing energy expenditure through its anorexic discharge, thus causing cachexia (Jun et al., 2023; Lin et al., 2013).

Molecular docking is a widely employed in silico technique to predict ligand-target interactions and assess the biological activity of natural products. It offers insights into protein or enzyme mechanisms and binding within their active sites., thus we employed this robust technique to elucidate the possible chemical entities that may have higher chances of binding with the pro-inflammatory cytokines. Our GC–MS analysis and molecular docking results supported the in-vivo results. Based on the dock score, we found two compounds with the lowest dock score. Hentriacontane docked in with IL-1β and IL-6 with −8.23, −8.18

respective dock scores, and palmitoyl amide docked in with TNF-α (-7.85). The anti-inflammatory effects of hentriacontane, found in this study, were also reported in RAW 264.7 cell line and Balb/c mice models at the doses of 1 μM, 5 μM and 10 μM (in-vitro experiments) and 1 mg/kg, 2 mg/kg, and 5 mg/kg (in-vivo experiments), which could be due to binding of this compound with these pro-inflammatory cytokines. They concluded hentriacontane as a potential anti-inflammatory candidate (Khajuria et al., 2017). Palmitoyl-ethanol amide was also reported to have anti-inflammatory activity, which is consistent with the results of this study (Impellizzeri et al., 2015). Joshi reported the GC–MS analysis of the axial parts of *C. bonplandianus* and found more than 96 % of the essential oils which contained about 40 compounds from these volatile oils. The sesquiterpenes was the most abundant hydrocarbon, while the main components were caryophyllene and germacrene D (Joshi, 2014).

In the arthritic group, histological analysis revealed an increase in pannus development, inflammatory cell infiltration, and bone resorption, consistent with findings from a previous study (Akhtar & Shabbir, 2019). No signs of inflammation were observed in the vehicle control group. However, a dose-dependent healing pattern was observed in the CBEE and CBAF treatments. Akhtar and Shabbir reported that all arthritis markers, including histopathological analysis and the gross arthritis score, were significantly reduced after treatment with *U. indica*

extracts and piroxicam. Piroxicam was used as the reference drug because it is commonly prescribed to individuals with arthritis to alleviate inflammation-related symptoms and modulate the immune system (Abdallah et al., 2011; Shabbir et al., 2014).

## 5. Conclusion

In conclusion, we observed that the *C. bonplandianus* ethanolic extract and aqueous fraction had anti-arthritic effects by minimizing edema, decreasing paw thickness, and restoring body weight. Additionally, these therapies restored abnormal blood parameters in treated rats. When compared to the arthritic control group, both the ethanol extract and aqueous fraction significantly showed downregulation of TNF-α, IL-6, and IL-1β. Moreover, the separation of necessary phytochemicals from CBEE and CBAF that oversee the anti-arthritic activity is extremely important. Furthermore, discovering other anti-inflammatory pathways is necessary. Clinical testing is recommended before using it as a nutraceutical. While studying the therapeutic effect of *C. bonplandianus*, it may be worth conducting research on osteogenic markers like RANKL.

## Author contributions

All authors contributed to the study conception and design. Material preparation, data collection and analysis were performed by Erum Javed, Hina Yasin, Qumar Shahzad and Zaheer Ul-Haq. The first draft of the manuscript was written by Erum Javed, Humaira Majeed Khan, Yasser Shahzad, Mobina Manzoor, Muhammad Usman Ghori, Amer M. Alanazi and Azmat Ali Khan, and all authors commented on previous versions of the manuscript. All authors read and approved the final manuscript.

## Declaration of competing interest

The authors declare that they have no known competing financial interests or personal relationships that could have appeared to influence the work reported in this paper.

## Acknowledgments

## References

Abdallah, F.I., Dawaba, H.M., Mansour, A., Samy, A.M., 2011. Evaluation of the antiinflammatory and analgesic effects of piroxicamloaded microemulsion in topical formulations. Int. J. Pharm. Pharm. Sci. 3 (2), 66–70.

Adebayo, S., Masoko, P., 2017. Therapeutic uses of plant species for inflammationrelated conditions in Limpopo province of South Africa: a mini-review and current perspectives. J. Pharmacogn. Phytother. 1, 2–8.

Ajoy, G., Padma, C., 2013. Brine shrimp cytotoxic activity of 50% alcoholic extract of Croton bonplandianum baill. Asian J. Pharm. Clin. Res. 6 (SUPPL.3), 40–41.

Akhtar, G., Shabbir, A., 2019. Urginea indica attenuated rheumatoid arthritis and inflammatory paw edema in diverse animal models of acute and chronic inflammation. J. Ethnopharmacol. 238, 111864 https://doi.org/10.1016/j.jep.2019.111864.

Aletaha, D., Smolen, J.S., 2018. Diagnosis and management of rheumatoid arthritis: a review. J. Am. Med. Assoc. 320 (13), 1360–1372.

Babu, N.P., Pandikumar, P., Ignacimuthu, S., 2011. Lysosomal membrane stabilization and anti-inflammatory activity of Clerodendrum phlomidis Lf, a traditional medicinal plant. J. Ethnopharmacol. 135 (3), 779–785.

Bar, G., Bar, M., 2020. Antibacterial efficiency of croton bonplandianum plant extract treated cotton fabric. Curr. Trends Fashion Technol. Text. Eng. 7, 5–9. https://doi.org/10.19080/CTFTTE.2020.07.555703.

Dutta, S., Chakraborty, A.K., Dey, P., Kar, P., Guha, P., Sen, S., Kumar, A., Sen, A., Chaudhuri, T.K., 2018. Amelioration of CCl4 induced liver injury in swiss albino mice by antioxidant rich leaf extract of Croton bonplandianus Baill. PLoS One 13 (4), e0196411.

Dutta, S., Chaudhuri, T.K., 2018. Pharmacological aspect of Croton bonplandianus Baill: A comprehensive review. J. Pharmacogn. Phytochem. 7 (1), 811–813.

Ekambaram, S., Perumal, S.S., Subramanian, V., 2010. Evaluation of antiarthritic activity of Strychnos potatorum Linn seeds in Freund's adjuvant induced arthritic rat model. BMC Complement. Altern. Med. 10, 1–9.

Gagné-Boulet, M., Bouzriba, C., Alvarez, A.C.C., Fortin, S., 2021. Phenyl 4-(2-oxopyrrolidin-1-yl) benzenesulfonates and phenyl 4-(2-oxopyrrolidin-1-yl) benzenesulfonamides as new antimicrotubule agents targeting the colchicine-binding site. Eur. J. Med. Chem. 213, 113136.

Ghosh, T., Biswas, M.K., Chatterjee, S., Roy, P., 2018. In-vitro study on the hemolytic activity of different extracts of Indian medicinal plant Croton bonplandianum with phytochemical estimation: a new era in drug development. J. Drug Deliv. Therap. 8 (4), 155–160.

Ghosh, T., Kumar Biswas, M., Roy, P., Guin, C., 2018. A Review on Traditional and Pharmacological Uses of Croton bonplandianum with Special Reference to Phytochemical Aspect. Eur. J. Med. Plants 22, 1–10. https://doi.org/10.9734/EJMP/2018/40697.

Hasan, U. H., Uttra, A. M., & Rasool, S. (2015). Evaluation of in vitro and in vivo anti-arthritic potential of Berberis calliobotrys. ||| *Bangladesh Journal of Pharmacology*, 10 (4), 807-819.

Impellizzeri, D., Ahmad, A., Bruschetta, G., Di Paola, R., Crupi, R., Paterniti, I., Esposito, E., Cuzzocrea, S., 2015. The anti-inflammatory effects of palmitoylethanolamide (PEA) on endotoxin-induced uveitis in rats. Eur. J. Pharmacol. 761, 28–35. https://doi.org/10.1016/j.ejphar.2015.04.025.

Joshi, R.K., 2014. Chemical composition of the essential oil of Croton bonplandianus from India. Nat. Prod. Commun. 9 (2), 269–270.

Jun, L., Robinson, M., Geetha, T., Broderick, T.L., Babu, J.R., 2023. Prevalence and mechanisms of skeletal muscle atrophy in metabolic conditions. Int. J. Mol. Sci. 24 (3), 2973.

Khajuria, V., Gupta, S., Sharma, N., Kumar, A., Lone, N.A., Khullar, M., Dutt, P., Sharma, P.R., Bhagat, A., Ahmed, Z., 2017. Anti-inflammatory potential of hentriacontane in LPS stimulated RAW 264.7 cells and mice model. Biomed. Pharmacother. 92, 175–186. https://doi.org/10.1016/j.biopha.2017.05.063.

Kumar, V., Verma, A., Ahmed, D., Sachan, N.K., Anwar, F., Pradesh, U., Hamdard, J., 2013. Fostered antiarthritic upshot of moringa oleifera lam. stem bark extract in diversely induced arthritis in wistar rats with plausible mechanism. Int. J. Pharm. Sci. Res. 4 (10), 3894–3901. https://doi.org/10.13040/IJPSR.0975-8232.4 (10).3894-01.

Kyei, S., Koffuor, G.A., Boampong, J.N., 2012. Antiarthritic effect of aqueous and ethanolic leaf extracts of Pistia stratiotes in adjuvant-induced arthritis in Sprague-Dawley rats. J. Exp. Pharmacol. 4, 41–51. https://doi.org/10.2147/JEP.S29792.

Lin, Y.-J., Anzaghe, M., Schülke, S., 2020. Update on the pathomechanism, diagnosis, and treatment options for rheumatoid arthritis. Cells 9 (4). https://doi.org/10.3390/cells9040880.

Lin, B., Zhang, H., Zhao, X.-X., Rahman, K., Wang, Y., Ma, X.-Q., Zheng, C.-J., Zhang, Q.-Y., Han, T., Qin, L.-P., 2013. Inhibitory effects of the root extract of Litsea cubeba (lour.) pers. on adjuvant arthritis in rats. J. Ethnopharmacol. 147 (2), 327–334.

Mahnashi, M. H., Jabbar, Z., Alamgeer, Irfan, H. M., Asim, M. H., Akram, M., Saif, A., Alshahrani, M. A., Alshehri, M. A., & Asiri, S. A. (2021). Venlafaxine demonstrated anti-arthritic activity possibly through down regulation of TNF-α, IL-6, IL-1β, and COX-2. *Inflammopharmacology*, 29, 1413-1425.

Mateen, S., Zafar, A., Moin, S., Khan, A.Q., Zubair, S., 2016. Understanding the role of cytokines in the pathogenesis of rheumatoid arthritis. Clin. Chim. Acta 455, 161–171. https://doi.org/10.1016/j.cca.2016.02.010.

Mo, J., Panichayupakaranant, P., Kaewnopparat, N., Nitiruangjaras, A., Reanmongkol, W., 2013. Topical anti-inflammatory and analgesic activities of standardized pomegranate rind extract in comparison with its marker compound ellagic acid in vivo. J. Ethnopharmacol. 148 (3), 901–908.

Moudgil, K.D., Venkatesha, S.H., 2022. The anti-inflammatory and immunomodulatory activities of natural products to control autoimmune inflammation. Int. J. Mol. Sci. 24 (1), 95.

Mustafa, G., Mahrosh, H. S., & Arif, R. (2021). In silico characterization of growth differentiation factors as inhibitors of TNF-alpha and IL-6 in immune-mediated inflammatory disease rheumatoid arthritis. *BioMed research international, 2021*.

Naz, R., Ahmed, Z., Shahzad, M., Shabbir, A., Kamal, F., 2020. Amelioration of rheumatoid arthritis by <i>Anacardium occidentale</i> via inhibition of collagenase and lysosomal enzymes. Evid. Based Complement. Alternat. Med. 2020, 8869484. https://doi.org/10.1155/2020/8869484.

Qaisar, M.N., Chaudhary, B.A., Sajid, M.U., Hussain, N., 2014. Evaluation of α-glucosidase inhibitory activity of dichloromethane and methanol extracts of croton bonplandianum baill. Trop. J. Pharm. Res. 13 (11), 1833–1836. https://doi.org/10.4314/tjpr.v13i11.9.

Rainsford, K.D., 2007. Anti-inflammatory drugs in the 21st century. Inflamm. Pathogen. Chronic Dis. 3–27.

Rajakaruna, N., Harris, C.S., Towers, G.H.N., 2002. Antimicrobial activity of plants collected from serpentine outcrops in Sri Lanka. Pharm. Biol. 40 (3), 235–244. https://doi.org/10.1076/phbi.40.3.235.5825.

Saggoo, M.I.S., Walia, S., Kaur, R., 2010. Evaluation of genotoxic and antimicrobial potential of Croton bonplandianum Baill. Arch. Appl. Sci. Res. 2 (2), 211–216.

Sangha, R.B., Gayatri, M.C., 2014. Ethanomedicinal properties of Euphorbiaceae family- a comprehensive review. Int. J. Phytmed. 6 (2), 144–156.

Sardar, M., Zia, K., Ashraf, S., Malik, H.N., Jabeen, A., Khan, K.M., Ul-Haq, Z., 2022. Interface inhibitory action on Interleukin-1β using selected anti-inflammatory compounds to mitigate the depression: A computational investigation. Comput. Biol. Chem. 101, 107774.

Scherer, H.U., Häupl, T., Burmester, G.R., 2020. The etiology of rheumatoid arthritis. J. Autoimmun. 110, 102400 https://doi.org/10.1016/j.jaut.2019.102400.

Sengar, N., Joshi, A., Prasad, S.K., Hemalatha, S., 2015. Anti-inflammatory, analgesic and anti-pyretic activities of standardized root extract of Jasminum sambac. J. Ethnopharmacol. 160, 140–148. https://doi.org/10.1016/j.jep.2014.11.039.

Shabbir, A., Shahzad, M., Ali, A., Zia-ur-Rehman, M., 2014. Anti-arthritic activity of N'-[(2,4-dihydroxyphenyl)methylidene]-2-(3,4-dimethyl-5,5-dioxidopyrazolo[4,3-c][1,2]benzothiazin-1(4H)-yl)acetohydrazide. Eur. J. Pharmacol. 738, 263–272. https://doi.org/10.1016/j.ejphar.2014.05.045.

Shabbir, A., Shahzad, M., Ali, A., Zia-Ur-Rehman, M., 2016. Discovery of new benzothiazine derivative as modulator of pro- and anti-inflammatory cytokines in rheumatoid arthritis. Inflammation 39 (6), 1918–1929. https://doi.org/10.1007/s10753-016-0427-y.

Simon, L.S., 2013. Nonsteroidal anti-inflammatory drugs and their risk: a story still in development. Arthritis Res. Ther. 15 (Suppl 3), 1–2.

Singha, R., Pattanayak, S., Kanthal, L.K., Jana, S., Bera, A., Dhang, A., Hazra, R., Pal, S., 2022. Evaluation of anthelmintic activity of methanolic extract of croton Bonplandianum Baill. Eur. J. Adv. Chem. Res. 3 (3), 40–44.

Sudha, T.R., 2021. Anti-inflammatory activity of aerial parts and root extracts of croton bonplandianum baill. Int. J. Sci. Develop. Res. 6 (4), 279–283.

Talwar, S., Nandakumar, K., Nayak, P.G., Bansal, P., Mudgal, J., Mor, V., Rao, C.M., Lobo, R., 2011. Anti-inflammatory activity of Terminalia paniculata bark extract against acute and chronic inflammation in rats. J. Ethnopharmacol. 134 (2), 323–328.

Uchikoga, N., Matsuzaki, Y., Ohue, M., Hirokawa, T., Akiyama, Y., 2013. Re-docking scheme for generating near-native protein complexes by assembling residue interaction fingerprints. PLoS One 8 (7), e69365.

Uttra, A.M., Hasan, U.H., 2017. Anti-arthritic activity of aqueous-methanolic extract and various fractions of Berberis orthobotrys Bien ex Aitch. BMC Complement. Altern. Med. 17, 1–16.

Uytan, G., Tokgöz, H.B., Ünal, R., Altan, F., 2021. Transcriptional analyses of the effects of Catharanthus roseus L. medicinal plant extracts on some markers related to obesity and inflammation in 3T3-L1 mouse cell lines. Biologia 76 (1), 297–306.

Weber, B.N., Giles, J.T., Liao, K.P., 2023. Shared inflammatory pathways of rheumatoid arthritis and atherosclerotic cardiovascular disease. Nat. Rev. Rheumatol. 1–12.

Wongrakpanich, S., Wongrakpanich, A., Melhado, K., Rangaswami, J., 2018. A comprehensive review of non-steroidal anti-inflammatory drug use in the elderly. Aging Dis. 9 (1), 143.

Woude, v. d. D., H.M, A., & Helm-van, M. (2018). Update on the epidemiology, risk factors, and disease outcomes of rheumatoid arthritis. *Best Practice & Research Clinical Rheumatology*, *32*(2), 174-187. https://doi.org/10.1016/j.berh.2018.10.005.

Yasin, H., Mahmud, S., Rizwani, G.H., Perveen, R., Abrar, H., Fatima, K., 2019. Effects of aqueous leaves extract of Holoptelea integrifolia (Roxb) Planch on liver and kidney histopathology of albino rats. Pak. J. Pharm. Sci. 32 (2), 569–573.

Yasin, H., Mahmud, S., Abrar, H., Arsalan, A., Jahan, N., Fatima, K., Bano, R., Hussain, R. A., Islam, M., 2021. Anti-inflammatory and histopathological studies of leaves extracts of Croton bonplandianus in Albino rats. Pak. J. Pharm. Sci. 34 (2), 747–753. https://doi.org/10.36721/PJPS.2021.34.2.SUP.747-753.1.

Zia, K., Ashraf, S., Jabeen, A., Saeed, M., Nur-e-Alam, M., Ahmed, S., Al-Rehaily, A.J., Ul-Haq, Z., 2020. Identification of potential TNF-α inhibitors: from in silico to in vitro studies. Sci. Rep. 10 (1), 1–9.